Vibrational Relaxation and Recombination of Nitrogen and Air in Hypersonic Nozzle Flows

H. T. NAGAMATSU* AND R. E. SHEER JR.†
General Electric Company, Schenectady, N. Y.

The effects of vibrational relaxation and recombination of high-temperature nitrogen and air were investigated in a hypersonic shock tunnel at high flow Mach numbers. The equilibrium temperature and pressure ranges after the reflected shock wave were 1400° to 7000°K and 100 to 500 psia. Static pressure measurements were made along the axis of the nozzle to determine the freezing of the vibrational mode during the expansion process. Vibrational relaxation times for nitrogen obtained from shock-tube experiments were used to calculate the relaxation length. Once the nitrogen vibrational mode freezes in the expansion region, there is very little exchange of the vibrational energy into the translational and rotational energies, and the static pressures are significantly lower than those calculated for an equilibrium expansion. The nonequilibrium effects for nitrogen are much less than those for air, and the large difference is caused mainly by the presence of oxygen. With air, the reservoir pressure has a large influence upon the departure from equilibrium expansion.

Introduction

As the vehicle velocity increases for long range ballistic missiles and satellites, the temperature behind the detached shock wave for a blunt body becomes very high. For a satellite, it is approximately 8500°K during re-entry at 100,000-ft alt. At these temperatures, air can no longer be considered as a simple diatomic molecule; instead chemical reactions, dissociation, and ionization occur. From the stagnation point of the blunt body, the gas will expand and cool, and the flow in the expansion process could proceed in equilibrium, "frozen," or nonequilibrium depending upon the initial pressure and temperature. At a temperature of 5000°K for nitrogen, there will be no dissociation, but the vibrational mode of nitrogen molecules is fully excited. Thus, by using nitrogen, it is possible to consider the vibrational relaxation and recombination separately at lower temperatures without any chemical reactions or ionization. With air in equilibrium at high temperatures, the number of species is very large as presented in Ref. 1.

The high-temperature gases used in hypersonic test facilities expand in the nozzle where chemical reactions, vibrational excitation, and recombination do play an important role for the determination of the state of the gas in the test section. Solutions have been obtained for the expansion of high-temperature air in a nozzle by assuming the flow to be one-dimensional and in thermodynamic equilibrium.[2,3] Experimentally,[2,4,5] it has been observed that air at reasonable temperatures and high enough pressures in the reservoir will expand very close to thermodynamic equilibrium in a hypersonic nozzle. The available experimental data on the expansion of dissociated gases in a nozzle or over a body are still very limited.

Numerous theoretical papers for the expansion of high-temperature gas in a nozzle are presented in Refs. 6–10. The equilibrium and nonequilibrium effects on the flow field have also been analyzed by a number of authors in recent years.[11–13] To solve the nonequilibrium flow problems, the authors usually relied upon the experimental data for the reaction rates[14–16] and vibrational relaxation times.[17,18] Very recent experiments on the vibrational relaxation times of nitrogen have resolved some of the effects of impurities and gas mixtures.

The present investigation was undertaken to study the vibrational relaxation times of nitrogen in the expansion region of a hypersonic nozzle and to obtain further experimental data for the nonequilibrium flow of dissociated air in the nozzle. Since it is possible to measure both the static and impact pressures along the axis of the nozzle, the thermodynamic state of the nitrogen can be analyzed from these two measurements. The impact pressure measurements[19] are rather insensitive to whether the gas expands in either a thermodynamic equilibrium or a "frozen" condition, and thus the effective area ratio can be determined for the nozzle at any given location. The static pressure measurements are greatly influenced by the state of the gas during the expansion process.

Description of Experiments

The tests were conducted in a hypersonic shock tunnel with a multiple nozzle arrangement. A detailed description of this facility and the associated instrumentation is presented in Ref. 20. The straight-through nozzle arrangement with a throat diameter of 1 in. and an exit diameter of 24 in. was used in the present study. To generate the high temperature at the entrance to the nozzle, a reflected shock wave from the end of the shock tube is used along with the combustion driver technique. By this method it is possible to produce compressed and heated gas for a period of several milliseconds.

The impact pressure along the axis of the nozzle was measured with a quartz piezoelectric pressure gage mounted inside a hemispherical nose piece having a radius of $\frac{3}{8}$ in. This impact pressure probe was calibrated dynamically in the 8-in.-diam calibration shock tube. Lead-zirconate-titinate piezoelectric pressure gages were mounted inside of a static pressure probe instead of the quartz gage because of the much higher output. Two static pressure probes, with diameters of $\frac{1}{2}$ and $\frac{3}{4}$ in. were used to measure the pressure along the nozzle axis. The output of these pressure gages was 30 and 100 mv/psi, respectively, as determined by a dynamic calibra-

Presented as Preprint 64-38 at the AIAA Aerospace Sciences Meeting, New York, January 20–22, 1964; revision received March 30, 1965. This research was partially supported by the Ballistic Systems Division, U. S. Air Force. The support of A. J. Nerad contributed to the attainment of results presented in this paper. Discussions with R. C. Millikan and D. R. White clarified the vibrational relaxation time of nitrogen. K. H. Cary assisted with the instrumentation, and G. W. Jones analyzed the nitrogen in the mass spectrometer.

* Research Associate, Mechanical Studies, Chemistry Research. Associate Fellow Member AIAA.

† Mechanical Engineer, Gas Dynamics, Mechanical Studies, Chemistry Research.

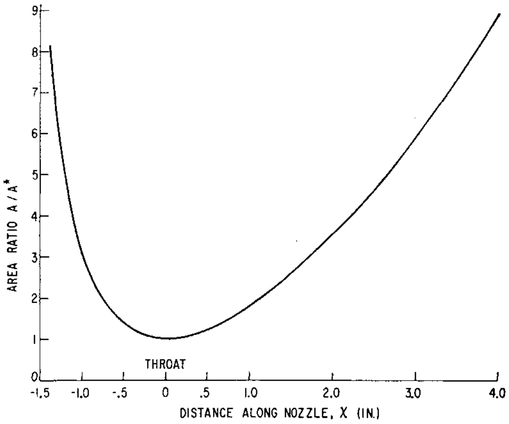

Fig. 1 Nozzle geometric area ratio near the throat.

tion. A detailed description of these slender static pressure probes is presented in Ref. 21.

The nitrogen used for the test gas was the Linde H. P. dry grade. A mass spectrometer analysis of a sample of nitrogen from the cylinder was made and results indicated nearly pure nitrogen with a small trace of water vapor. For experiments with air, the building supply air of standard composition with a dew point of $-80°F$ was used to charge the driven tube. The driven tube was evacuated, flushed with the test gas, and evacuated once more before the final charging.

The pressure P_5 behind the reflected shock wave at the entrance to the nozzle is measured with a standard Kistler quartz gage. The corresponding reflected stagnation temperature T_5 is calculated by using the measured shock velocity at the end of the driven tube, the initial pressure and temperature in the tube, and the thermodynamic data for nitrogen presented in Refs. 22–24, and those for air presented in Refs. 1 and 25.

Solutions for Equilibrium and Frozen Nozzle Flow

A. Equilibrium Flow

The equilbrium flow conditions in the nozzle have been calculated for nitrogen using the Mollier diagram presented in Ref. 22. By using the data presented in Refs. 23 and 24, the equilibrium reflected flow conditions were determined.

To investigate the freezing of the vibrational mode in the throat region for nitrogen, the equilibrium flow calculations

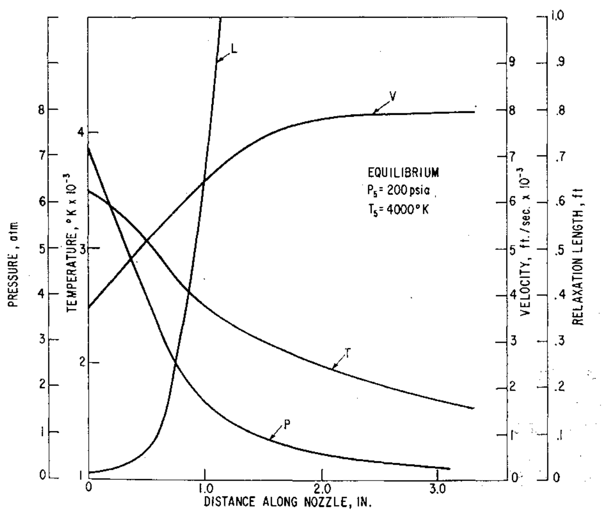

Fig. 2 Calculated equilibrium nozzle flow properties for nitrogen with P_5 = 200 psia and T_5 = 4000°K.

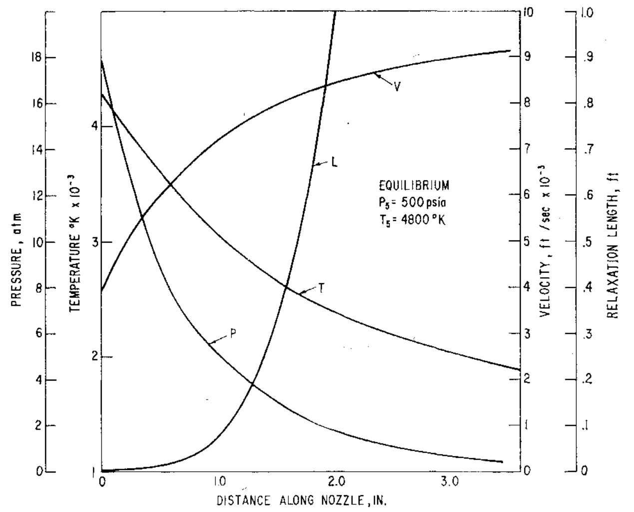

Fig. 3 Calculated equilibrium nozzle flow properties for nitrogen with P_5 = 500 psia and T_5 = 4800°K.

were made for the following reflected stagnation conditions: P_5 = 200 psia and T_5 = 4000°K; P_5 = 500 psia and T_5 = 4800°K; P_5 = 100 psia and T_5 = 6000°K. These particular reservoir conditions were selected to indicate the effects of pressure and temperature upon the vibrational relaxation in the nozzle and to correlate with the experimental data. By assuming the nitrogen to be in equilibrium at all stations as a first approximation, it is possible to determine the pressure, temperature, density, and velocity as a function of x for a particular nozzle geometry. The nozzle geometry used is shown in Fig. 1. These calculated equilibrium results are presented in Figs. 2–4. Because of the relatively high reservoir pressures, the expansion process was analyzed starting from the throat region. This procedure assumed that the high-temperature nitrogen was in vibrational equilibrium at the throat and the calculated values of the relaxation distance, $L = \tau v$, have indicated that the assumption was correct. In calculating the relaxation distance, the equilibrium velocity and the relaxation time τ given in Ref. 18, based upon the equilibrium pressures and temperatures, were used to determine the relaxation length as a function of the distance.

Since the relaxation time is inversely proportional to the pressure and is highly dependent on the temperature, the relaxation length at the throat is greatest for P_5 = 200 psia and T_5 =

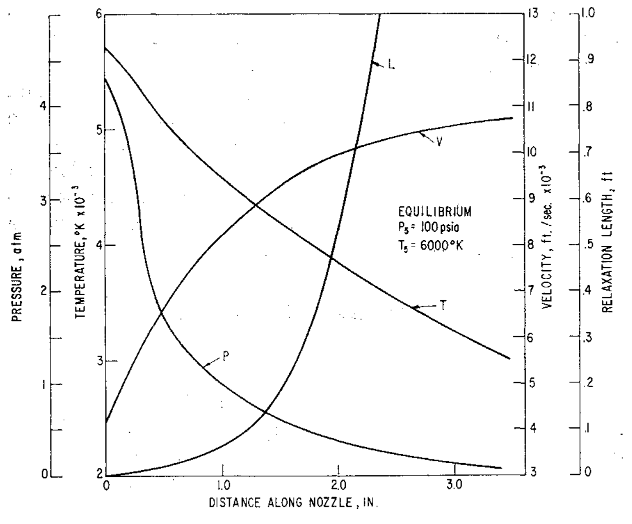

Fig. 4 Calculated equilibrium nozzle flow properties for nitrogen with P_5 = 100 psia and T_5 = 6000°K.

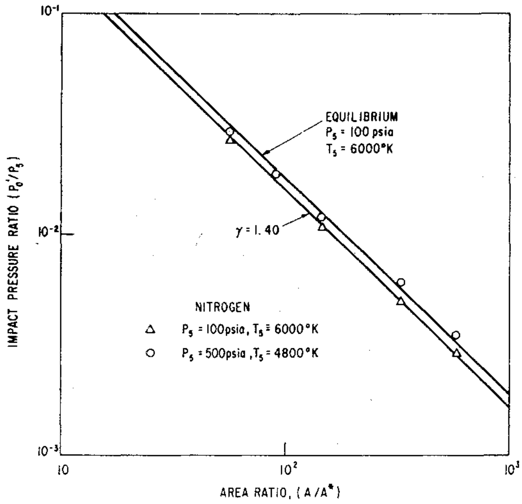

Fig. 5 Impact pressure ratio as a function of geometric area ratio for nitrogen.

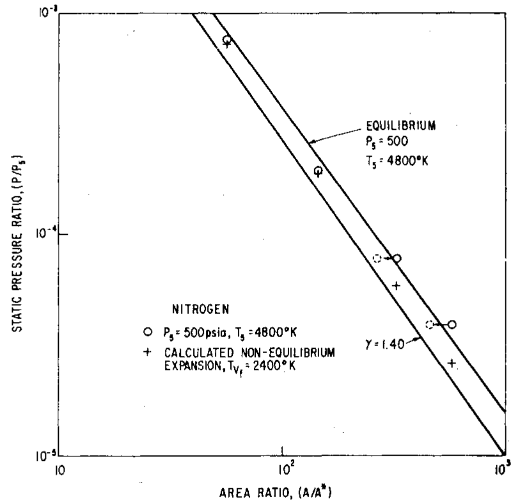

Fig. 6a Static pressure ratio as a function of geometric area ratio for nitrogen, P_5 = 500 psia and T_5 = 4800°K.

$4000°K$ as indicated by comparing Figs. 2–4. The relaxation length calculated on the basis of equilibrium nozzle flow as a first approximation increases very rapidly with the distance from the throat. The effects of pressure and temperature upon the relaxation length are illustrated by the three reservoir conditions presented in these figures.

In Figs. 5 and 6, the equilibrium static and impact pressures have been calculated for nitrogen as a function of area ratio for reflected reservoir conditions of $P_5 = 100$ psia and $T_5 = 6000°K$, and $P_5 = 500$ psia and $T_5 = 4800°K$. In these figures the results for a perfect gas condition with $\gamma = 1.40$ have been plotted as a comparison. The observed experimental static and impact pressure measurements are plotted to indicate the correlation with the calculated data.

The ratio of the static pressure in the nozzle to the reflected pressure at the entrance to the nozzle (P/P_5) has been calculated for an area ratio of 144 as a function of reflected stagnation temperature T_5 for reservoir pressures of 100 and 1000 psia for nitrogen. These results are plotted in Figs. 7a–7c, together with the experimental data.

The Mollier diagram for air, presented in Ref. 25, was used to calculate the equilibrium flow conditions in the nozzle. In Figs. 7a–7c, the calculated equilibrium static pressure ratios are presented for an area ratio of 144 at reflected pressures of 100, 300, and 1000 psia.[2]

B. Frozen Flow

For the condition of no chemical reactions or dissociation, the frozen flow for the vibrational mode was calculated by assuming the flow to be the same as the perfect gas flow with constant γ and a reservoir temperature equal to T_5. When chemical reactions, dissociation, and ionization existed in the reservoir for equilibrium conditions, the frozen flow was calculated by using the effective ratio of specific heats defined in Ref. 2. This method was used to determine the flow parameters for the assumption of frozen flow, and the results are presented in Figs. 5–7 for nitrogen and air.

Results and Discussion

A. Nitrogen

In Figs. 2–4, the equilibrium flow parameters have been calculated for reflected stagnation conditions of P_5 = 200 psia and T_5 = 4000°K, P_5 = 500 psia and T_5 = 4800°K, P_5 = 100 psia and T_5 = 6000°K. The temperatures are high enough for the first two reservoir conditions, so that only translational, rotational, and vibrational modes must be considered during the expansion process, whereas for the 6000°K case,

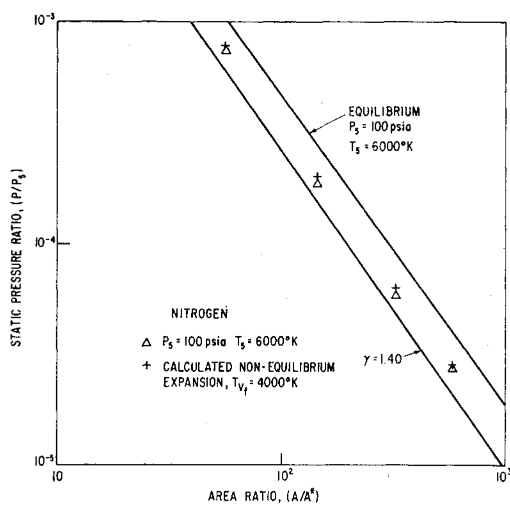

Fig. 6b Static pressure ratio and function of geometric area ratio for nitrogen, P_5 = 100 psia and T_5 = 6000°K.

the nitrogen is vibrationally excited as well as having some dissociation present. For these reservoir conditions, the relaxation lengths at the throat are all much less than the throat diameter as indicated in Figs. 2–4. However, farther downstream, the relaxation length increases rapidly so that freezing is to be expected.

For the nonequilibrium flow in the nozzle, an approximate method was used to obtain the solution. It was assumed as a first approximation that the flow in the nozzle was in equilibrium at all nozzle stations. From the relaxation lengths calculated for the equilibrium condition, the vibrational freezing point was selected to correspond with the portion of the curve where $dL/dx \gg 1$. In Table 1, the flow properties at the assumed location in the nozzle for freezing of the vibrational mode are presented for the three selected reservoir conditions. Up to the beginning of the vibrational freezing, the flow in the nozzle was assumed to be in equilibrium. Beyond the freezing point, the gas was assumed to be a perfect gas with the constant specific heat ratio of 1.40, which assumes that there is no exchange of vibrational energy into translational and rotational modes for the molecules. The nonequilibrium static pressure ratios, calculated as a function of the area ratio by this method for the two reservoir conditions, are presented in Figs. 6a and 6b, together with the calculated equilibrium curves and the experimental data.

The measured static pressure ratio and the calculated nonequilibrium values are presented in Fig. 6a for a reflected stagnation condition of 500 psia at 4800°K. Also in this figure, the curves for calculated equilibrium and perfect gas with $\gamma = 1.40$ are plotted. The agreement between the calculated and measured static pressure ratios for a geometric area ratio of 56.1 and 144 are in good agreement because of the relatively small boundary-layer displacement effects as indicated by the impact pressure measurements at these two locations (Fig. 5). At area ratios of 324 and 576, the impact measurements have indicated that the nozzle boundary-layer effects are significant. In Fig. 5, the calculated equilibrium and frozen impact pressure distribution, as a function of area ratio, was very close to the results predicted by the perfect gas case $\gamma = 1.40$. From the impact measurements at these two stations, the effective nozzle area ratio can be determined by comparing the measured values with the predicted values for an inviscid flow condition. The measured static pressure ratios at these larger area ratios lie above the calculated equilibrium value for an inviscid flow as indicated in Fig. 6a. By using the effective area ratios determined from the measured impact pressures, the static pressure ratios were corrected in Fig. 6a. With this correction, the experimental static pressure ratios again agree well with the nonequilibrium calculated values. In the calculation, the vibrational temperature at freezing was taken to be 2400°K. The corresponding translational and rotational temperature in the test section with a geometric diameter of 24 in. is 308°K for the nonequilibrium flow assumption. The good agreement between the calculated and experimental static pressures indicates that the vibrational energy will remain frozen during the expansion with very little exchange of the vibrational energy to the translational and rotational mode.

For a reservoir condition of 100 psia at 6000°K, the agreement between the calculated nonequilibrium static pressure ratios and the experimental data is surprisingly good (Fig. 6b). Both of these static pressure ratios are much less than that predicted by assuming equilibrium flow in the nozzle. The impact pressure results, for this condition as a function of area ratio, are presented in Fig. 5. The experimental data agreed very closely with the curve calculated for a perfect gas condition with $\gamma = 1.40$, which corresponds very closely to the impact pressure variation for nonequilibrium flow.

Because of the relatively cool wall temperature as compared to the stagnation temperature, the impact pressure measurements indicate that the boundary layer on the nozzle wall was relatively thin. This is probably one of the reasons why there was a good agreement between the measured static pressure ratios and the calculated nonequilibrium values. In the test section at the 24-in. nozzle diameter, the calculated ambient translational and rotational temperature is 446°K, whereas the vibrational temperature was assumed to be frozen at 4000°K near the throat of the nozzle. Since the measured and calculated nonequilibrium static pressure ratios are in good agreement, there seems to be very little exchange of vibrational energy into the translational and rotational modes for the nitrogen molecules during the expansion over a distance of approximately four feet. Thus, if the pressure and temperature are low enough in the nozzle, the vibrational relaxation will cause the vibrational temperature to be much greater than the gas temperature in the hypersonic nozzle. This is not in agreement with the results for the vibrational temperature determined optically in Ref. 26.

Table 1 Flow properties at assumed vibrational freezing location

P_5, psia	T_5, °K	X_f, in.	T_{vf}, °K	L, ft
200	4000	1.14	2420	1.05
500	4800	1.97	2400	1.02
100	6000	1.86	4000	0.41

With the static pressure probe located at the 12-in.-diam station, which corresponds to an area ratio of 144, the reflected stagnation pressures and temperatures were varied with nitrogen. Reflected pressures of 100, 200, and 500 psia were selected for the present investigation, and the reflected stagnation temperatures varied from approximately 2000° to 7000°K. Since the nozzle analysis for nonequilibrium required a great deal of numerical calculation, only these reservoir conditions were analyzed to determine the static pressure ratios at an area ratio of 144, and the nonequilibrium calculated values are presented in Figs. 7a–7c. For a reservoir

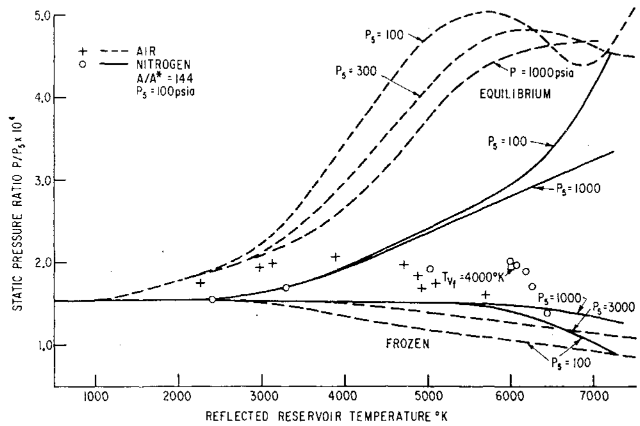

Fig. 7a Variation of static pressure ratio with reservoir temperature for nitrogen and air, P_5 = 100 psia.

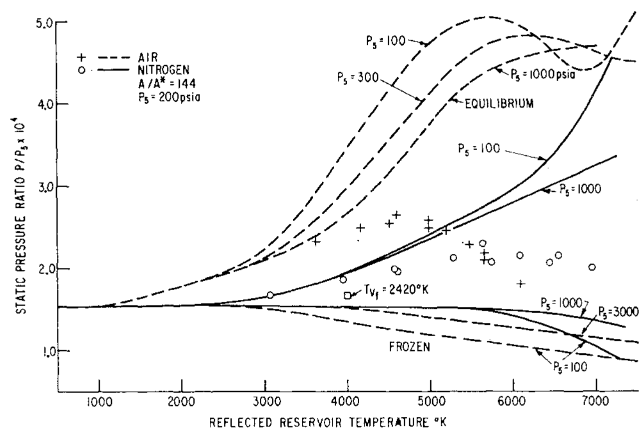

Fig. 7b Variation of static pressure ratio with reservoir temperature for nitrogen and air, P_5 = 200 psia.

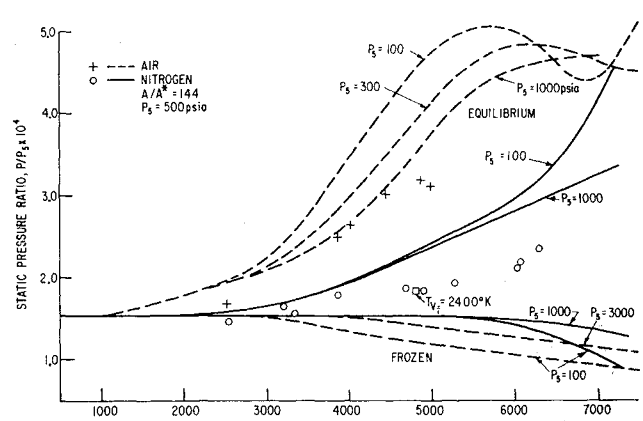

Fig. 7c Variation of static pressure ratio with reservoir temperature for nitrogen and air, P_5 = 500 psia.

pressure of 100 psia and temperature of 6000°K, with vibrational freezing temperature of 4000°K, the calculated nonequilibrium static pressure agrees very closely with the experimental data as indicated in Fig. 7a. This indicates that the vibrational energy is frozen at the value close to the above freezing temperature. The measured static pressures tend toward the completely frozen case for temperatures greater than 6000°K because of the vibrational and dissociation freezing during the expansion process.

The measured static pressure ratios for a reflected pressure of 200 psia are presented in Fig. 7b, together with the calculated equilibrium and frozen values. For a reflected stagnation temperature of 4000°K, the freezing was assumed to occur at a vibrational temperature of 2420°K (Fig. 2). The calculated nonequilibrium static pressure ratio for this freezing temperature is presented in Fig. 7b. Because this calculated value is less than the experimental data, the vibrational freezing temperature must be slightly less than the assumed temperature. There is a significant decrease in the static pressure from the equilibrium value because of the freezing of the vibrational mode downstream of the throat in the nozzle. At temperatures greater than 5000°K both vibrational and dissociation freezing occur in the nozzle.

In Fig. 7c, the static pressure ratios for a reflected pressure of 500 psia are plotted and compared with the calculated equilibrium and frozen curves. At a reflected stagnation temperature of 4800°K, the temperature for vibrational freezing was assumed to be 2400°K (Fig. 3). The corresponding calculated nonequilibrium static pressure ratio at an area ratio of 144 is plotted in Fig. 7c and agrees well with the experimental data.

B. Air

In Ref. 2, the static pressure ratios for air as functions of reflected stagnation temperature and pressure were obtained several years ago with barium-titinate pressure gages. It was decided to repeat these earlier experiments with more sensitive lead-zirconate-titinate pressure gages that have an output nearly twice that of barium-titinate.

The results of the static pressure measurements at an area ratio of 144 for air at reflected stagnation pressures of 100, 200, and 500 psia for various reflected temperatures are presented in Figs. 7a–7c. In these figures the calculated equilibrium and frozen values are plotted for different reflected pressures. It can be seen that the real gas effects for air are much greater than for nitrogen because of the presence of oxygen. The present data for the static pressure measurements agree within the experimental accuracy with the results presented in Refs. 2 and 4. For a reflected pressure of 100 psia, the flow departs from equilibrium expansion at a temperature of approximately 2500°K, and at 5700°K the static pressure ratio is approximately one-third of the theoretical equilibrium value. This large departure is caused by the low recombination rates for air at low pressure because of the lack of a sufficient number of collisions between the air species to maintain equilibrium during the expansion process.

For a reflected pressure of 200 psia, the expansion of air is close to equilibrium up to a reflected temperature of approximately 3000°K. The maximum static pressure ratio occurs at a stagnation temperature of about 4500°K before decreasing rapidly toward the frozen value with increasing temperature. At a temperature of 6100°K, the measured static pressure ratio was much lower than the equilibrium value indicating that appreciable freezing had occurred during the expansion in the nozzle. At the highest reflected pressure of 500 psia, the static pressure ratios did not depart significantly from the equilibrium values up to a temperature of approximately 4500°K. For the same reservoir pressure of 500 psia and temperature of 4500°K, the measured static pressure ratio for air is about 50% greater than that for nitrogen. With nitrogen at this particular temperature, only the vibrational mode is excited without any dissociation in the reservoir.

In Ref. 4, the experimental data for the static pressure ratios have been compared with the calculated values. Using the best estimates for the recombination rates and for a reservoir pressure of 500 psia, the calculated nonequilibrium values are appreciably lower than the experimental data at high temperatures. Since the experimental results for air obtained in the present investigation as well as those presented in the forementioned references do not agree with the nonequilibrium calculations, further investigations must be conducted to determine the reasons for the disagreement.

Conclusions

Static pressure probes with piezoelectric gages are sensitive enough to detect the freezing of the vibrational mode of energy during the expansion process of high temperature gases in a hypersonic nozzle. The impact pressure measurements can be used to determine the effective area ratio for the nozzle.

The vibrational relaxation times for nitrogen obtained by White and Millikan from infrared and interferometric data in shock tubes were used to calculate the relaxation length from which the freezing point in the nozzle was determined.

Once the nitrogen vibrational mode freezes in the expansion region, there is very little exchange of vibrational energy into the translational and rotational energies. The frozen vibrational temperature is much higher than the translational and rotational temperatures in the test section.

The nonequilibrium flow characteristics can be determined by assuming the flow to be in equilibrium up to the freezing point and beyond that point the flow can be considered to be frozen with a constant ratio of specific heats. The calculated nonequilibrium values agreed closely with the experimental data.

For air, the reservoir pressure has a large influence upon the departure from equilibrium expansion, so that air expands close to equilibrium at a reservoir temperature of 4500°K and 500 psia. Further experimental and theoretical investigations must be conducted to increase the knowledge regarding the expansion of high temperature gases in a hypersonic nozzle, as well as over bodies re-entering the planetary atmospheres at high velocities.

References

[1] Gilmore, F. R., "Equilibrium composition and thermodynamic properties of air to 24,000°K," Rand Corp. RM-1543 (August 1955).

[2] Nagamatsu, H. T., Workman, J. B., and Sheer, R. E., Jr., "Hypersonic nozzle expansion of air with atom recombination present," J. Aerospace Sci. **28**, 833–837 (1961).

[3] Erickson, W. D. and Creekmore, H. S., "A study of equilibrium real gas effects in hypersonic air nozzle, including charts of thermodynamic properties for equilibrium air," NASA TN D-231 (1960).

[4] Geiger, R. E., "Experimental investigations of the aerodynamic effects on non-equilibrium in inviscid blunt body flows," General Electric Space Sciences Lab., Rept. 62SD925 (1963).

[5] Duffy, R. E., "Experimental study of nonequilibrium expanding flows," AIAA J. **3**, 237–244 (1965).

[6] Bray, K. N. C., "Atomic recombination in a hypersonic wind tunnel nozzle," J. Fluid Mech. **6**, 1–32 (1959).

[7] Li, T. Y., "Non-equilibrium flow in gas dynamics," Air Force Office of Scientific Research TN 59-389 (1959).

[8] Vincenti, W. G., "Calculations of the one-dimensional nonequilibrium flow of air through a hypersonic nozzle—interim report," Arnold Engineering Development Center AEDC-TN-61-65 (1961).

[9] Hall, J. G., Eschenroeder, A. Q., and Marrone, P. V., "Inviscid hypersonic air flows with coupled non-equilibrium processes," IAS Preprint 62-67 (January 1962).

[10] Emanuel, G., "Problems underlying the numerical integration of the chemical and vibrational rate equations in a near-equilibrium flow," Arnold Engineering Development Center AEDC-TDR-63-82 (1963).

[11] Lighthill, M. J., "Dynamics of a dissociating gas, Part I—Equilibrium flow," J. Fluid Mech. 2, 1–32 (1957).

[12] Lenard, M., Long, M. E., and Wan, K. S., "Chemical non-equilibrium effects in hypersonic pure air wakes," ARS Preprint 2675-62 (December 1962).

[13] Whalen, R. J., "Viscous and inviscid non-equilibrium gas flow," IAS Preprint 61-23 (January 1961).

[14] Mathews, D. L., "Interferometric measurement in the shock tube of the dissociation rate of oxygen," Phys. Fluids 2, 170–178 (1959).

[15] Byron, S. B., "Interferometric measurement of the rate of dissociation of oxygen heated by strong shock waves," J. Chem. Phys. 30, 1380–1392 (1959).

[16] Lin, S. C. and Teare, J. D., "Rate of ionization behind shock waves in air, II. Theoretical interpretation," Avco Research Rept. 115 (1962).

[17] Blackman, V., "Vibrational relaxation in oxygen and nitrogen," J. Fluid Mech. 1, 61–85 (1956).

[18] Millikan, R. C. and White, D. R., "Vibrational energy exchange between N_2 and CO; The vibrational relaxation of nitrogen," J. Chem. Phys. 39, 98–101 (1963).

[19] Nagamatsu, H. T., Geiger, R. E., and Sheer, R. E., Jr., "Real gas effects in flow over blunt bodies at hypersonic speeds," J. Aerospace Sci. 27, 241–251 (1960).

[20] Nagamatsu, H. T., Geiger, R. E., and Sheer, R. E., Jr., "Hypersonic shock tunnel," J. ARS 29, 332–340 (1959).

[21] Nagamatsu, H. T., Sheer, R. E., Jr., Osburg, L. A., and Cary, K. H., "Design features of the General Electric Research Laboratory hypersonic shock tunnel," General Electric Research Lab. Rept. 61-RL-2711C (1961).

[22] Humphrey, R. L., Little, W. J., and Seeley, L. A., "Mollier diagram for nitrogen," Arnold Engineering Development Center AEDC-TN-60-83 (1960).

[23] Alpher, R. A. and Greyber, H. D., "Calculation of shock hugoniots and related quantities for nitrogen and oxygen," Phys. Fluids 2, 160–161 (1958).

[24] Smith, C. E., Jr., "Thermodynamic properties of nitrogen," Lockheed Missiles and Space Co., Rept. 6-90-62-111 (1962).

[25] Hilsenrath, J. and Beckett, C. W., "Tables of thermodynamic properties of argon-free air to 15,000°K," Arnold Engineering Development Center TN-56-12 (1956).

[26] Hurle, I. R., Russo, A. L., and Hall, J. G., "Experimental studies of vibrational and dissociative nonequilibrium in expanded gas flows," AIAA Preprint 63-439 (1963).

AUGUST 1965 AIAA JOURNAL VOL. 3, NO. 8

Hypersonic Viscous Effects on Free-Flight Slender Cones

BAIN DAYMAN JR.*

Jet Propulsion Laboratory, California Institute of Technology, Pasadena, Calif.

An experimental study was performed in order to determine the effects of various parameters upon cone aerodynamics in the hypersonic regime at Reynolds numbers as low as 7800/in. The use of free-flight models eliminated the need for evaluating sting interference and made practical accurate measurement of drag forces down to 8×10^{-4} lb and pitching moments as low as 2×10^{-4} in-lb. The effects of model to total temperature ratios of 0.45 (gun launch) and 0.87 (wire release) for 6° through 15° half-angle cones on total drag and static stability were investigated at Mach numbers from 6 to 10 for values of the viscous Knudsen number up to $M_\infty/(R_{D\infty})^{1/2} = 0.28$. Limited nose-blunting effects were also investigated. Conical shock viscous drag theory agrees quite favorably with the experimental data. Use is made of trends predicted by theory in order to compare the data of this paper with available hypersonic viscous cone drag data.

Nomenclature

A = model base area
C_f = flat-plate local skin-friction coefficient
C_{DT} = total effective drag coefficient of oscillating model = drag/$q_\infty A$ (no correction for base pressure)
C_{D0_T} = total drag coefficient at zero angle of attack = $C_{DT} - \epsilon\alpha_{\text{env}}^2$, deg^2
ΔC_{D_v} = viscous interaction drag = $C_{D0_T} - [C_{D0_T}]$ at $\bar{V}_\infty' = 0$
C_{m_α} = effective pitching moment slope/rad = moment/$q_\infty AD$
C_{N_α} = normal force coefficient slope/rad = (normal force)/$q_\infty A$
C_c = cone-surface form of Chapman-Rubesin viscosity coefficient = $\mu_w T_c/\mu_c T_w$
C_∞ = freestream form of Chapman-Rubesin viscosity coefficient = $\mu_w T_\infty/\mu_\infty T_w$
D = model base diameter
K = hypersonic viscous parameter (based on model length) = $M_\infty/(R_{L\infty})^{1/2}$
K' = hypersonic viscous parameter (based on model base diameter) = $M_\infty/(R_{D\infty})^{1/2}$
L = model length (for blunted models, length taken as that for sharp-nose model of same diameter)
M = Mach number
P = pressure
P_0' = freestream pitot pressure
q = dynamic pressure
r = radius
Re/in. = Reynolds number/in.
R_D = Reynolds number based on model base diameter
R_L = Reynolds number based on model length, L
R_x = Reynolds number based on distance from flat-plate leading edge
t = time
T = temperature
$\bar{V}$ = hypersonic viscous parameter = $M(C/R_L)^{1/2}$
$\bar{V}'$ = hypersonic viscous parameter = $M(C/R_D)^{1/2}$
V_m = model velocity relative to ground
$X_{c.g.}$ = distance of c.g. aft from model nose (sharp)
$\bar{\chi}_L$ = hypersonic viscous interaction parameter = $M_c^3(C_c/R_{Lc})^{1/2}$
α = angle of attack
α_{env} = envelope of oscillation
β = slope of drag curve (based on model length) = dC_{D0_T}/dK
β' = slope of drag curve (based on model base diameter) = dC_{D0_T}/dK'

Presented as Preprint 64-46 at the AIAA Aerospace Sciences Meeting, New York, N.Y., January 20–22, 1964; revision received April 14, 1965. This paper presents the results of one phase of research carried out at the Jet Propulsion Laboratory, California Institute of Technology, under Contract No. NAS 7-100, sponsored by NASA.

* Manager, Aerodynamic Facilities Section. Associate Fellow Member AIAA.